24. Hybrid system of nickel–cobalt hydroxide on carbonised natural cellulose materials for supercapacitors / Jiang L., Shanmuganathan S., Nelson G. W., Han S. O., Kim H., Na Sim I., Foord J. S. // Journal of Solid State Electrochemistry. 2017. Vol. 22, Issue 2. P. 387–393. doi: 10.1007/s10008-017-3723-z
25. Self-Stacked Reduced Graphene Oxide Nanosheets Coated with Cobalt-Nickel Hydroxide by One-Step Electrochemical Deposition toward Flexible Electrochromic Supercapacitors / Grote F., Yu Z.-Y., Wang J.-L., Yu S.-H., Lei Y. // Small. 2015. Vol. 11, Issue 36. P. 4666–4672. doi: 10.1002/smll.201501037
26. Micka K., Zábranský Z., Svatá M. Optimisation of active material for positive electrodes of Ni-Cd accumulators // Journal of Power Sources. 1982. Vol. 1, Issue 1. P. 9–16. doi: 10.1016/0378-7753(82)80003-7
27. Ten'kovtsev V. V., Tsenter B. I. Osnovy teorii i ekspluatatsii germetichnyh nikel'- kadmievyh akkumulyatorov. Leningrad: Energoatomizdat, 1985. 93 p.
28. Study on the reduction behavior of CoOOH during the storage of nickel/metal-hydride battery / Li X., Xia T., Dong H., Wei Y. // Materials Chemistry and Physics. 2006. Vol. 100, Issue 2-3. P. 486–489. doi: 10.1016/j.matchemphys.2006.01.031



***Проведено теоретичні та експериментальні дослідження можливостей використання гібридного лазерно-ультразвукового зміцнення та оздоблювання металевих виробів. Запропоновано методику для оцінки градієнту температур при використанні сканувального лазерного променя та ультразвукового інструменту. Визначено температуру початку деформаційної дії ультразвуковим інструментом в процесі термодеформаційного зміцнення та оздоблювання великогабаритних сталевих поверхонь***



***Ключові слова: лазерно-ультразвукове зміцнення, сталь 45, термокінетична модель, термофізична модель, твердість, шорсткість***



***Проведены теоретические и экспериментальные исследования возможностей использования гибридного лазерно-ультразвукового упрочнения и отделки металлических изделий. Предложена методика для оценки градиента температур при использовании сканирующего лазерного луча и ультразвукового инструмента. Определена температура начала деформационного действия ультразвуковым инструментом в процессе термодеформационного упрочнения и отделки крупногабаритных стальных поверхностей***



***Ключевые слова: лазерно-ультразвуковое упрочнение, сталь 45, термокинетическая модель, термофизическая модель, твердость, шероховатость***

UDC 621.9.048.7 : 621.9.048.6
DOI: 10.15587/1729-4061.2018.124031


# SURFACE HARDENING AND FINISHING OF METALLIC PRODUCTS BY HYBRID LASER-ULTRASONIC TREATMENT


**V. Dzhemelinskyi**
PhD, Professor*
E-mail: vitaly.dzhemelinsky@gmail.com
**D. Lesyk**
PhD, Assistant*
E-mail: lesyk_d@ukr.net
**O. Goncharuk**
PhD, Associate Professor*
E-mail: goncharuk.alex@gmail.com
**O. Danyleiko**
Postgraduate student*
E-mail: danyleiko.oleksandr@gmail.com
*Depatment of Laser System and Physical Technologies
National Technical University of Ukraine
"Igor Sikorsky Kyiv Polytechnic Institute"
Peremohy ave., 37, Kyiv, Ukraine, 03056


## 1. Introduction

The surface hardening is one of the effective ways to increase the wear resistance of parts in modern production due to changes in the chemical composition, modification, as well as changes in the surface microrelief and the structure of the surface layer. Given that a large number of machine parts work in extreme conditions, traditional surface hardening methods often do not allow getting the required qualitative indicators that fully meet the operation conditions. Moreover, the use of high-strength materials is often economically unprofitable.

Laser or plasma surface treatment is used to solve these problems in production processes. It should be noted that the laser surface hardening technology allows treating complex shaped parts with minimal zones of thermal influence in comparison with traditional processes (induction, flame and bulk hardening) [1–3]. Currently, laser surface hardening is successfully used to improve the wear resistance of responsible parts [4]. It is known that the combined method of surface-plastic deformation (SPD) is carried out after laser heat treatment (LHT) under a separate scheme at ambient temperature. In contrast to the combined method, the

hybrid method of thermo-deformation surface hardening is realized under a combined scheme when the heated surface is subjected to the SPD during cooling. The combination of certain types of surface hardening allows getting a much greater effect in improving wear resistance, reliability and durability of products. The prediction of the advantages and disadvantages of combined/hybrid methods of surface hardening are the basis for choosing the most effective one.

Thereby, the development of new surface hardening methods of metallic products with the use of combined and hybrid energy sources becomes especially relevant.

## 2. Literature review and problem statement

In the study [5], the shot-peening of the surface layer of X5CrNiCuNb 16-4 steel using a $CO_2$ laser after the LHT has been used. The results showed that the microhardness of the near-surface layer increased from 580 HV to 913 HV after deformation action. Herewith, the magnitude of the compressive residual macrostresses reached –600...1000 MPa. Another technological solution is the use of plasma-carburizing in combination with shot-peening [6] or deep-rolling [7]. It should be noted that the use of deep-rolling ($Ra$~0.1 μm) as finishing treatment [6] can significantly improve the surface roughness compared to the shot-peening ($Ra$~1.7 μm) [7]. The use of shot-peening allows processing of complex shaped metallic parts, which can not always be processed with deep-rolling. However, these methods do not allow getting the desired surface roughness.

Unlike the combined treatment, the hybrid treatment consists in using the-thermal energy of the laser beam (plasma arc) and the mechanical energy of the deformation tool. It is known that there is a more intense grain refinement and an increase in the defect density in the structure when using the hybrid thermo-deformation hardening of AISI 1045 steel by a continuous $CO_2$ laser and deforming tool in the form of a roller. Herewith, the compressive residual macrostresses are formed (–400...500 MPa) in the surface layer [8]. As a result, the fatigue strength and the wear resistance of the hardened layer increased by 30...80% and 10 times, respectively, compared to the initial state. Additionally, in comparison with the untreated surface, surface roughness decreases almost twice after the hybrid thermal-deformation treatment [9]. Nevertheless, it should be noted that the use of roller as the deforming tool does not allow the implementation of the SPD of complex profile parts.

Combined and hybrid methods of laser/plasma surface hardening using the SPD with the energy of ultrasonic oscillations are more promising. The combination of laser high-speed heating of materials combined with ultrasonic impact treatment (UIT) can be implemented in a different technological sequence, which affects the final outcome of treatment. Currently, combined thermo-deformation hardening is carried out using both mono-pin [10] and multi-pin [11] ultrasonic tools, depending on the type of the treated surface. In particular, the ultrasonic burnishing process is commonly used to treat the cylindrical surfaces. In this case, the hardened layer is characterized by both high hardness (~650 HV) and low surface roughness ($Ra$~0.15 μm) [10]. In the work [11], the realization possibilities of the combined laser-ultrasonic hardening of flat-shaped parts using a high-power fiber laser and multi-pin ultrasonic tool have been shown. The results confirmed that the combined LHT+UIT increases the wear resistance of the hardened layer at least two times due to the formation of a fine-grained structure with high hardness [12] and microrelief with low roughness [13].

In the application of LHT combined with UIT of the surface that is not cooled, the formation of martensite occurs from pre-plastically deformed austenite, which inherited the dislocation and structural arrangement [14]. As a result, the dispersion of the structural components, the density of dislocations, the strength and hardness of the surface layer increase. Futhermore, the compressive residual stresses and microrelief on the surface are formed after the UIT process. In comparison with the LHT+SPD, the preliminary SPD before the laser [15] or plasma [16] treatment allows preparing the structure for high-temperature processing, increasing the depth and microhardness of the hardened layer compared to the separate thermal treatment.

Thus, laser-deformation surface treatment of steels can be realized on different stages of the temperature-time cycle of cooling of the treated surface. In particular, in conditions of high-temperature, medium-temperature and low-temperature deformation (hybrid treatment) or in conditions of deformation at ambient temperature (combined treatment).

## 3. The aim and objectives of the study

The aim of this work is to determine the beginning temperature of intense SPD in the cooling process of the surface heated by a scanning laser beam. This will make it possible to implement the surface hardening and finishing of metallic products by hybrid laser-ultrasonic treatment.

To achieve the aim, let us consider the following objectives:

– to determine the heating temperature range of the treated surface by the scanning laser beam without melting and to calculate the critical points of structural-phase transformations in the LHT of AISI 1045 steel using the thermo-kinetic model;

– to compare the results of experimental studies of the surface heating temperature measured by a pyrometer with the determined magnitude of the heating temperature using the thermo-physical model of the LHT, as well as to estimate the deformation heating in the UIT;

– to conduct a comparative analysis of surface roughness and microhardness of the surface layer after the LHT, UIT, combined and hybrid LHT+UIT.

## 4. Materials and methods of the study

### 4. 1. Material and description of applied surface treatments

The studies were carried out on flat specimens 20 mm in thickness of AISI 1045 steel. Preliminary, the specimens were annealed and polished.

The LHT of the specimens was carried out using a milling center with computer numerical control (CNC), a fiber laser, a scanner and a temperature control system [17, 18]. A detailed description of the equipment used is given in [11–13]. The LHT was conducted in the following regimes: heating temperature of 900...1,300 °C, LHT speed of 40...140 mm/min, scanning speed of 1,000 mm/s, scanning width of 10 mm [11].

Preliminary, the analysis of the LHT was carried out using the diagrams of heating/cooling cycles of AISI 1045 steel and state diagram of Fe-C. Moreover, the calculation of temperature critical points of structural-phase transformations of the investigated steel was carried out using the thermo-kinetic model [1]. The thermo-physical model [19] was used to assess/verify the temperature gradient with the experimental data, which were measured by the pyrometer.

The thermo-deformation hardening of the specimens was carried out using both combined and hybrid treatment. The hybrid treatment scheme is shown in Fig. 1. The processed specimen is simultaneously heated by the scanning laser beam of dimensions $b_{sc}\times l_{sc}$ with maintaining a constant temperature determined in real time by the pyrometer and deformed by a dynamic tool located at a distance of $l$. The distance between the spots of the thermal and deformation tools depends primarily on the shape of the laser beam and the design of the deforming tool, as well as on the properties of the treated steel and the regimes of LHT and UIT.

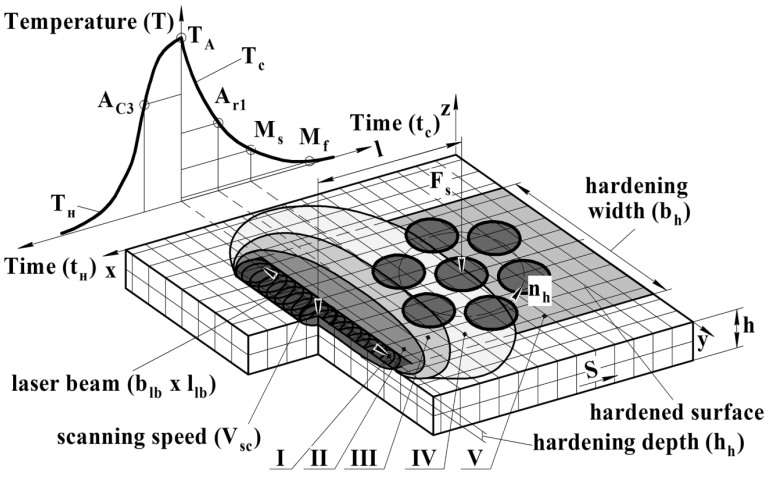


Fig. 1. Design scheme of hybrid LHT+UIT: *I* – the austenite formation zone (high-temperature zone), II – the austenite decomposition zone, III – the medium-temperature deformation zone, IV – the low-temperature deformation zone (martensite formation zone), V – the zone of LHT+UIT

The UIT was performed using a CNC machine, an ultrasonic generator and an ultrasonic vibration system that contained a piezoceramic transducer, a waveguide horn and a multi-pin impact head [11, 20, 21]. The UIT regimes: the amplitude and frequency of ultrasonic horn are 18 μm and 21.6 kHz, respectively, the static load of the ultrasonic tool is 50 N and the rotational speed of the impact head is 79 rpm.

**4. 2. Thermo-kinetic model of laser heat treatment**

To determine the complete austenization temperature range ($T>A_{C1}/A_{C3}$) and the beginning and end temperature of the martensitic transformation, the following experimental models were used [1, 22]:

$$A_{C3} = 910 - 370C - 27.4Mn - \\ -27.3Si - 6.35Cr - 32.7Ni + ... - 60.2V^2, \quad (1)$$

$$M_s = 561 + 474C - 33Mn - 17.7Ni - \\ -12.1Cr - 7.5Mo + 10Co - 705Si, \quad (2)$$

$$M_f = M_s - 215, \quad (3)$$

where $A_{C3}$, $M_s$, $M_f$ are the temperature critical points of structural-phase transformations of steels, °C; C, Mn, Cr, Si, Ni, V,... is the chemical composition of the material, %.

**4. 3. Thermo-physical model of laser heat treatment**

For modeling the LHT process by the scanning laser beam (Fig. 2) and estimating the temperature distribution $T(x, y, z, t)$ in the depth and on the surface of the specimen, a three-dimensional nonlinear heat equation [19, 22–24] was used:

$$c\rho\frac{\partial T}{\partial t} = \frac{\partial}{\partial x}\left(\lambda\frac{\partial T}{\partial x}\right) + \frac{\partial}{\partial y}\left(\lambda\frac{\partial T}{\partial y}\right) + \frac{\partial}{\partial z}\left(\lambda\frac{\partial T}{\partial z}\right), \quad (4)$$

where $T$ is the surface temperature of the specimen material at a coordinate point $(x, y, z)$ at the time $t\in(0, T_k)$; $\rho$ is the density of the specimen material, kg/m$^3$; $c(T)$ is the coefficient of heat capacity of the specimen material, J/kg·°C; $\lambda(T)$ is the coefficient of thermal conductivity of the specimen material, W/m·°C; $l$, $b$, $h$ are the length, width and height of the specimen, respectively, cm.

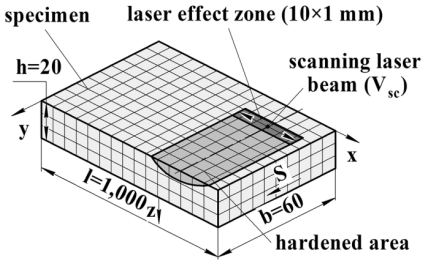


Fig. 2. Scheme of the LHT by scanning laser beam

Numerical simulation of temperature distribution on the processed specimen was realized according to the formula (4) by the finite difference method with the following boundary conditions. In particular, at the moment of time ($t$=0), the initial specimen temperature is equal to the ambient temperature of $T_s^0 = 20$ °C, and the initial state of the specimen was described $T(x,y,z,0) = T_s^0$. Herewith, the boundary condition on the treatment surface in the zone of laser radiation was described [19]:

$$\lambda\frac{\partial T(x,y,0,t)}{\partial z} + W_{lb}(x,y,t) = 0, \quad (5)$$

where the right-hand side of equation (5) represents the heat flux ($W_{lb}$), which is perpendicular to the laser scanning direction (W/m$^2$).

In this model, the boundary conditions of the laser beam were considered in the form of a rectangular shape of the action zone (1×0.1 cm) (Fig. 2), which has a uniform distribution of the radiation power density $W_{lb}$:

$$W_{lb} = AP / h_{lb}l_{lb}, \quad (6)$$

where $A$ is the absorption coefficient of the surface, $P$ is the laser power, W; $h_{lb}$ is the width of the laser beam (1 cm), $l_{lb}$ is the length of the laser beam (0.1 cm).

In the calculations, the following thermo-physical characteristics of AISI 1045 steel were used: ρ=7,800 kg/m$^3$,

$c$=473 J/kg·°C, λ=50 W/m·°C, α=2.3·10$^{-5}$ m$^2$/s, $T^0$=20 °C, $A$=0.8. The evaluation of the temperature gradients both on the surface and in the depth of the bulk specimen was carried out by means of the finite difference method using the software developed [19]. At a heating temperature (1,200 °C) of AISI 1045 steel, the average calculated laser power was 680, 690, 730 W at a specimen feed rate of 0.06, 0.15, 0.23 cm/s, respectively.

**4. 4. Determination of temperature in ultrasonic impact treatment**

An approximate solution of the plane thermo-elasticity problem [25] was used for the analysis of the UIT at the contact of multi-pin impact head (AISI 52100 steel) with the treated surface (AISI 1045 steel) (Fig. 3).

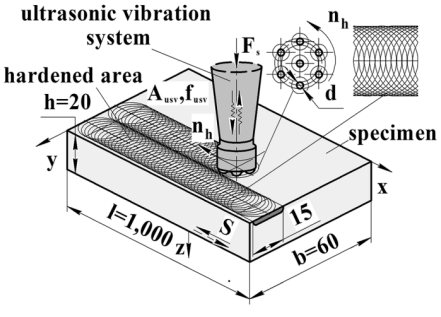


Fig. 3. Scheme of UIT by multi-pin impact head

Herewith, the deformation heating distribution $\Delta T(z)$ of the surface layer in the specimen depth was estimated taking into account the Peclet criteria, which characterize the ratio of the total amount of heat that occurs at the moment of the impact loading by the pins of the metallic surface at depth $z$ [25]:

$$\Delta T(z)=1/Pe^{+}\times$$
$$\times\left\{f(y)+(Pe^{-}T^0_{ust}+2(1-K_0)\sqrt{Pe_s}T^0_s)\cdot erfc\left(z/2\sqrt{\tau_{us}}\right)\right\}+T^0_{ust}, \quad (7)$$

$$f(y)=2\sqrt{\pi/\tau_{us}}\exp\left(-z^2/4\tau_{us}\right)-z\cdot erfc\left(z/2\sqrt{\tau_{us}}\right),$$

$$Pe^{\pm}=K_0\sqrt{Pe_{ust}}\pm(1-K_0)\sqrt{Pe_s},$$

$$K_0=(\lambda_{ust}/(\lambda_{ust}+\lambda_s)), Pe_{ust}=$$
$$=2d_c\rho_s/\alpha_{ust}, Pe_s=2d_c\rho_{ust}/\alpha_s,$$

where $Pe_{ust}$, $Pe_s$ are the Peclet criteria for the ultrasonic tool and the specimen, $T^0_{ust}$ and $T^0_s$ is the initial temperature of the pins and the specimen, °C; $\rho_{ust}$ and $\rho_s$ is the density of the pins material and the specimen, kg/m$^3$; $d_c$ is the diameter of the contact area, m; $\tau_{us}$ is the duration of UIT (s), which was determined according to the formula $\tau_{us}=d_c/S$.

## 5. Results of the research of the beginning temperature determination of intense SPD

The following equation (1)–(3) was used to determine the temperature critical points of structural-phase transformations ($A_{C1}$=712 °C, $A_{C3}$=784 °C, $A_{r1}$=603 °C, $A_{r3}$=710 °C, $M_s$= =358 °C, $M_f$=243 °C). The calculated temperature critical points of structural-phase transformations of AISI 1045 steel allowed preliminary to predict the heating temperature range of the surface layer by the scanning laser beam at LHT speeds of 50...150 mm/min (Fig. 4), avoiding melting.

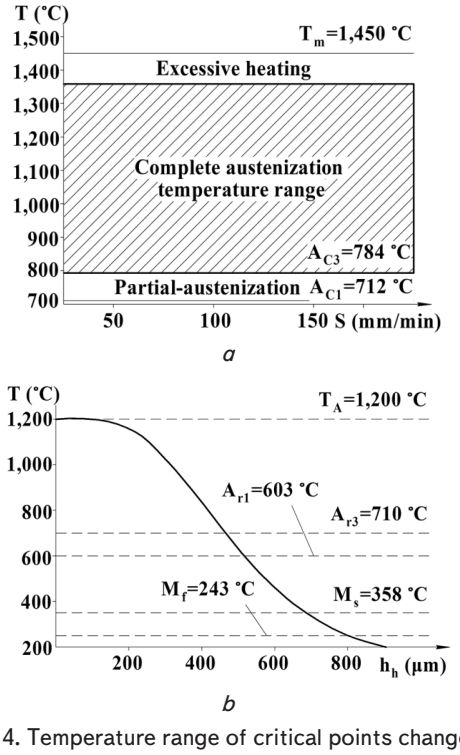


Fig. 4. Temperature range of critical points change of AISI 1045 steel: *a* — the formation of austenite; *b* — the formation of martensite with temperature distribution in the specimen depth at the LHT speed of 90 mm/min

The calculations of the temperature gradients both on the surface and in the specimen depth were carried out using special software by the finite difference method [19, 22, 23]. The calculated magnitude of the laser beam power was approximately 690 W at the heating temperature of 1,200 °C and the LHT speed of 90 mm/min (Fig. 5). Herewith, the calculated power density was in the range of $10^3$...$10^4$ W/cm$^2$ with the laser exposure duration of ~0.5 s, which provided surface thermal hardening without surface melting. Fig. 4, *b* shows that the determined magnitude of temperature on the treated surface correlates well with the temperature measured by the laser pyrometer (Fig. 5), which beam was focused in the center of the laser track. Moreover, Fig. 5 shows that higher laser power should be provided at the beginning of the LHT. Almost constant laser power in the intermediate zone of the laser track is observed after reaching the required temperature on the treated surface. The laser power decreases when the laser beam reaches the edge of the treated surface (Fig. 5, point B).

Thus, the used process of measuring and controlling the heating temperature in the laser beam area is sufficiently accurate. On the other hand, the magnitudes of the laser beam power obtained in the LHT by maintaining a constant temperature allow estimating the amount of laser beam energy consumed to achieve the required heating temperature.

Herewith, it was found that the laser power increases proportionally with the increase in the feed rate of the treated specimen (Fig. 6, *a*). The hardening depth and microhardness of the surface layer grow with increasing heating temperature (Fig. 6, *b*). In particular, the depth of the hardened

layer is 350...450 μm at a heating temperature of 1,300 °C and the specimen feed rate of 40...90 mm/min. Despite the high hardness in the near-surface layer (~900 HV), melting zones and cracks were not found in it. However, a further increase in temperature can lead not only to an increase in the hardening depth, but also a decrease in the surface hardness and the melting of the microasperities peaks of the treated surface, which is not permissible in the manufacture of end products.

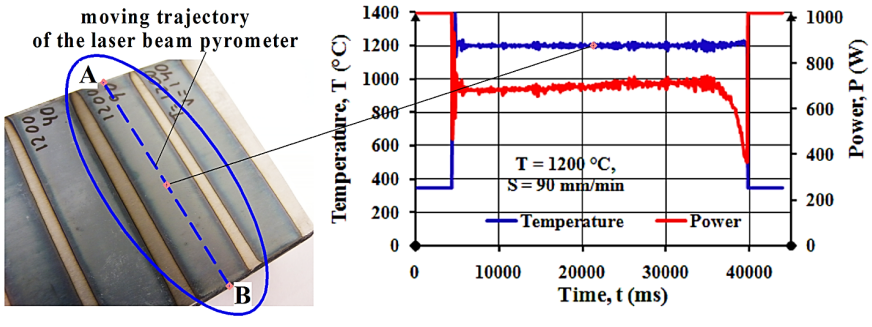


Fig. 5. Variation the laser power at a heating temperature of 1,200 °C and specimen feed rate of 90 mm/min

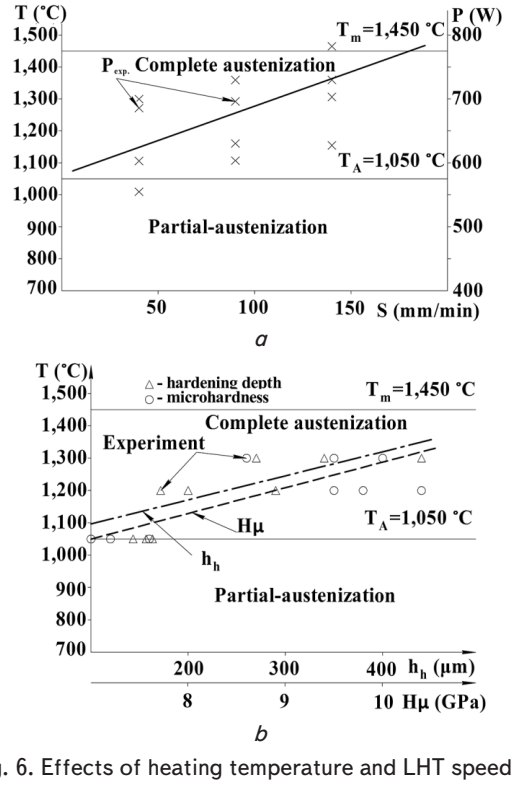


Fig. 6. Effects of heating temperature and LHT speed on: *a* — the change of laser power; *b* — the change in the hardening depth and microhardness of the surface layer

Thus, the above obtained results of experimental and theoretical studies allowed narrowing the range of optimum LHT regimes using the fiber laser and scanner.

The surface temperature in the UIT was determined to implement the combined or hybrid laser-ultrasonic hardening and finishing process. The results of the calculation according to formulas (7) allowed both calculating the temperature distribution along the depth of the specimen and estimating the deformation heating temperature on the treated surface, which was ~40 °C (Fig. 7).

Thus, the additional deformation heating of the surface by the tip is ~50 °C in the UIT with a multi-tip impact head allows expanding the temperature range of the hybrid thermo-deformation hardening and finishing.

In Fig. 8, the results of temperature distribution on the specimen surface from time, when carbon steel AISI 1045 was hardened by the scanning laser beam, based on experimental data of temperature change from time by means of measuring the heating (cooling) temperature by the pyrometer is given. In this case, the zone of deformation action was finally determined taking into account theoretical calculations of the magnitude of the beginning and end temperature of the martensitic transformation during the specimen cooling.

The deformation treatment of large-sized surfaces of products by the multi-pin ultrasonic tool heated by the scanning laser beam provides a high specific number of impacts at different cooling temperatures. In particular, applying the extreme working surface of the multi-pin ultrasonic tool at a cooling temperature in the range of 400...550 °C (Fig. 8, point O) will contribute to the change in the structural components in a still heated state of the surface layers after the preliminary laser heating [8, 19] and simultaneous improvement of the parameters of the surface microrelief [9]. Additionally, the start of the martensitic transformation is slowed down by about 2...3 s due to the deformation heating of the surface ~50...100 °C.

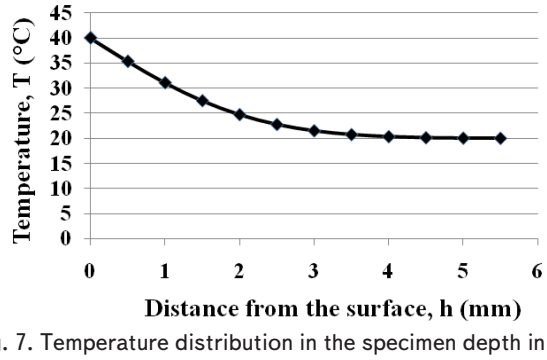


Fig. 7. Temperature distribution in the specimen depth in UIT of AISI 1045 steel

It should be noted that at a large distance between the laser beam and the ultrasonic tool, applying the hybrid laser-ultrasonic treatment is inappropriate because of intermediate deformation of the treated surface before martensitic transformation. To reduce the distance between the laser beam and the ultrasonic tool, it is necessary to install a scanner in the hand of the robot, which will allow focusing the laser beam at a slight angle (6...12°) to the treated surface, providing a distance of 8...10 mm. This distance corresponds to a cooling temperature of ~500 °C between the extreme working surfaces of the pin and the laser beam.

The results of experimental studies have established that hybrid treatment provides the greatest microhardness of the surface layer (Fig. 9) and the lowest surface roughness

(Fig. 10). However, it was found that a surface profile with a larger surface wavelength is formed after the hybrid treatment (Fig. 9) due to the intense plastic deformation of the surface in a still heated state.

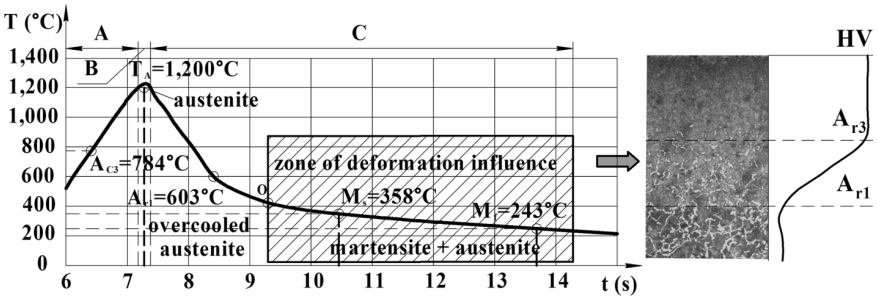


Fig. 8. Calculation-experimental dependence of the heating and cooling surface temperature of AISI 1045 steel on time in the LHT with the deformation action zone: A – austenization, B – homonization, C – quenching and SPD, O – extreme point of the working surface of deformation tool

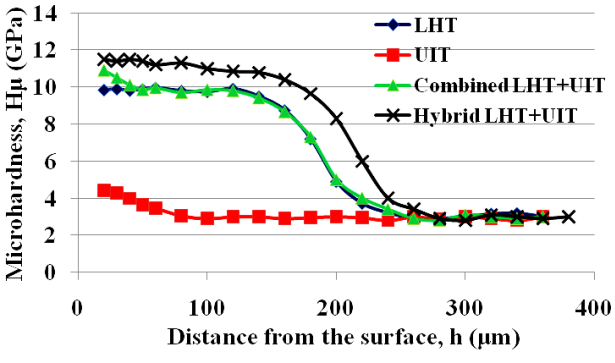


Fig. 9. Microhardness distribution in the depth of the surface layer of AISI 1045 steel after LHT, UIT, combined and hybrid LHT+UIT

In comparison with the initial state, the hybrid laser-ultrasonic treatment allowed increasing the surface hardness more than 3 times and reducing the roughness parameter *Ra* approximately 3 times (Fig. 9, 10). Herewith, the hardening is deeper compared to the combined treatment.

Furthermore, in contrast to the combined treatment, the hybrid laser-ultrasonic treatment provides a more even microhardness distribution in the near-surface layer (Fig. 9).

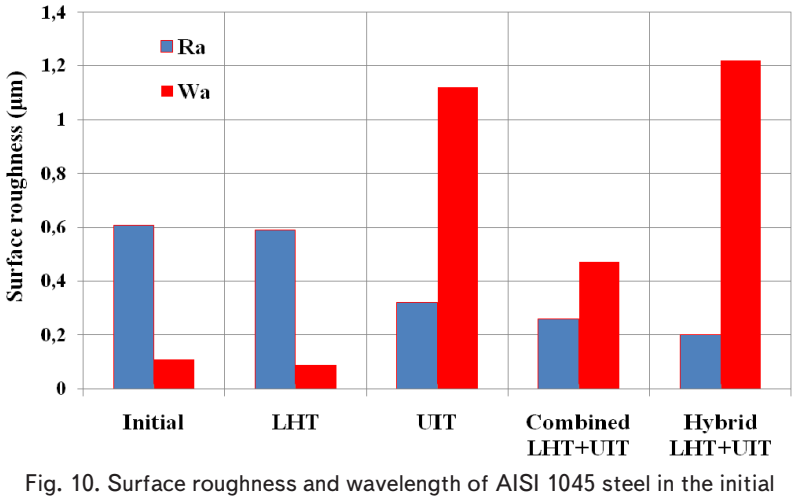


Fig. 10. Surface roughness and wavelength of AISI 1045 steel in the initial state and after LHT, UIT, combined and hybrid LHT+UIT

## 6. Discussion of surface hardening and finishing of metallic products by hybrid LHT+UIT

It should be noted that the identified critical points of austenite and martensite formation temperature at the heating/cooling stage of the hypo-eutectoid steel by the laser beam (Fig. 4) correlate well with the known works [1, 22]. As a consequence, this allows reducing the range of optimum LHT regimes using the fiber laser and scanning optics, providing high hardness and required hardening depth of the surface layer (Fig. 6, *b*).

Moreover, the previous theoretical and experimental studies of the temperature gradient separately both for the LHT and the UIT (Fig. 4, 7, 8) allowed determining the magnitude of the cooling temperature and the distance from the center of the laser beam to the point of applying the deformation tool. The determined magnitudes are in good agreement with the work [19], where the authors implement the hybrid thermo-deformation method of surface hardening of AISI 1045 steel using the $CO_2$ laser and roller.

The results of experimental studies have confirmed that in comparison with the applied methods of surface hardening, the lower surface roughness and the highest hardness of the treated surface are after the hybrid laser-ultrasonic treatment. Moreover, it should be noted that the roughness parameter *Ra* is smaller after the hybrid LHT+UIT (*Ra*~0.2 μm) than after the hybrid thermo-deformation hardening process using a Nd:YAG laser and roller (*Ra* 0.5...1 μm) [9]. Herewith, the magnitudes of the surface hardness and the hardening depth of the surface layer are twice as much after the proposed hybrid LHT+UIT method.

Thus, the use of ultrafast laser heating and cooling of materials combined with the SPD process by the multi-pin ultrasonic tip will allow the formation of hardening layers with fine-grained structures and guaranteed residual compressive macrostresses [12]. This allows increasing the operational properties of the responsible large-sized parts, which work in extreme conditions.

It should be noted that in comparison with the hybrid treatment, the combined laser-ultrasonic treatment can successfully be used both for treatment of small-sized and large-sized parts, especially of the complex profile. On the other hand, the implementation of the proposed hybrid laser-ultrasonic process of hardening and finishing of metallic large-sized products in manufacturing requires additional costs in the first stage of technology application.

The determination of the influence of the beginning temperature of deformation hardening depending on the type of the treated material is planned in more detail in order to apply the hybrid LHT+UIT in manufacturing. Additionally, it is necessary to conduct a study of microstructural patterns and their impact on the operational properties.

## 7. Conclusions

1. The austenization temperature range (1,050... 1,350 °C) at different speeds (50...150 mm/min) of LHT without surface melting by the scanning laser beam, as well as the beginning temperature of the martensitic transformation (~360 °C) during the specimen cooling were determined.

2. It is shown that the determined magnitude of temperature on the specimen surface of AISI 1045 steel by means of the thermo-physical model correlates well with the heating temperature (1,200 °C) measured by the pyrometer. The beginning temperature (400...550 °C) of the intense SPD of steel products and the application distance (8...10 mm) of the multi-pin ultrasonic tool during the specimen cooling were determined.

3. It was found that the proposed hybrid LHT+UIT allowed increasing the microhardness of surface layers more than 3 times and reducing the roughness parameter *Ra* approximately 3 times compared to the initial state, provided favorable conditions to trap oil on the product surface.

## Acknowledgements

The authors of the article are grateful to Prof. A. Lamikiz and Dr. S. Martinez (University of the Basque Country, Bilbao, Spain), as well as Dr. B. N. Mordyuk and Dr. G. I. Prokopenko (G. V. Kurdyumov Institute for Metal Physics of the NAS of Ukraine, Kyiv, Ukraine) for the given opportunity of carrying out the experimental study.

References

1. Santhanakrishnan S., Dahotre N. B. Laser surface hardening // ASM Handbook Volume 4A: Steel Heat Treating Fundamentals and Processes. 2013. P. 476–491.
2. Kovalenko V., Zhuk R. Systemized approach in laser industrial systems design // Journal of Materials Processing Technology. 2004. Vol. 149, Issue 1-3. P. 553–556. doi: 10.1016/j.jmatprotec.2004.02.020
3. The study of the influence of laser hardening conditions on the change in properties of steels / Idan A. F. I., Akimov O., Golovko L., Goncharuk O., Kostyk K. // Eastern-European Journal of Enterprise Technologies. 2016. Vol. 2, Issue 5 (80). P. 69–73. doi: 10.15587/1729-4061.2016.65455
4. Klocke F., Schulz M., Gräfe S. Optimization of the Laser Hardening Process by Adapting the Intensity Distribution to Generate a Top-hat Temperature Distribution Using Freeform Optics // Coatings. 2017. Vol. 7, Issue 12. P. 77. doi: 10.3390/coatings7060077
5. Influence of shot peening on the fatigue life of laser hardened 17-4PH steel / Wang Z., Jiang C., Gan X., Chen Y., Ji V. // International Journal of Fatigue. 2011. Vol. 33, Issue 4. P. 549–556. doi: 10.1016/j.ijfatigue.2010.10.010
6. Tsuji N., Tanaka S., Takasugi T. Effects of combined plasma-carburizing and shot-peening on fatigue and wear properties of Ti–6Al–4V alloy // Surface and Coatings Technology. 2009. Vol. 203, Issue 10-11. P. 1400–1405. doi: 10.1016/j.surfcoat.2008.11.013
7. Tsuji N., Tanaka S., Takasugi T. Effect of combined plasma-carburizing and deep-rolling on notch fatigue property of Ti-6Al-4V alloy // Materials Science and Engineering: A. 2009. Vol. 499, Issue 1-2. P. 482–488. doi: 10.1016/j.msea.2008.09.008
8. Lazerne termodeformatsiyne zmitsnennia detalei silskohospodarskykh mashyn / Mazheika A. I., Chaikovskyi O. B., Mukhammed A. Sh. M., Lutai A. M. // Konstruiuvannia, vyrobnytstvo ta ekspluatatsiya silskohospodarskykh mashyn. 2006. Issue 1. P. 140–146.
9. Tian Y., Shin Y. C. Laser-assisted burnishing of metals // International Journal of Machine Tools and Manufacture. 2007. Vol. 47, Issue 1. P. 14–22. doi: 10.1016/j.ijmachtools.2006.03.002
10. Effect of ultrasonic nanocrystal surface modification on the fatigue behaviors of plasma-nitrided S45C steel / Wu B., Wang P., Pyoun Y.-S., Zhang J., Murakami R. // Surface and Coatings Technology. 2012. Vol. 213. P. 271–277. doi: 10.1016/j.surfcoat.2012.10.063
11. Surface microrelief and hardness of laser hardened and ultrasonically peened AISI D2 tool steel / Lesyk D. A., Martinez S., Dzhemelinskyy V. V., Lamikiz A., Mordyuk B. N., Prokopenko G. I. // Surface and Coatings Technology. 2015. Vol. 278. P. 108–120. doi: 10.1016/j.surfcoat.2015.07.049
12. Microstructure related enhancement in wear resistance of tool steel AISI D2 by applying laser heat treatment followed by ultrasonic impact treatment / Lesyk D. A., Martinez S., Mordyuk B. N., Dzhemelinskyi V. V., Lamikiz A., Prokopenko G. I. et. al. // Surface and Coatings Technology. 2017. Vol. 328. P. 344–354. doi: 10.1016/j.surfcoat.2017.08.045
13. Laser-Hardened and Ultrasonically Peened Surface Layers on Tool Steel AISI D2: Correlation of the Bearing Curves' Parameters, Hardness and Wear / Lesyk D. A., Martinez S., Mordyuk B. N., Dzhemelinskyi V. V., Lamikiz A., Prokopenko G. I. et. al. // Journal of Materials Engineering and Performance. 2017. Vol. 27, Issue 2. P. 764–776. doi: 10.1007/s11665-017-3107-7
14. Brover A. V. Strukturnoe sostoyanie poverhnostnyh sloev stali X12M posle lazerno-akusticheskoy obrabotki // Vesnik Mashinostroeniya. 2008. Issue 11. P. 67–69.

15. Gureev D. M. Laser-ultrasonic hardening of steel surface // Adv. Cond. Matt. Mater. Research. 2001. Vol. 3, Issue 1. P. 87–94.
16. Residual Stress, Structure and Other Properties Formation by Combined Thermo-Hardening Processing of Surface Layer of Gray Cast Iron Parts / Rakhimyanov K. M., Nikitin Y. V., Semenova Y. S., Eremina A. S. // IOP Conference Series: Materials Science and Engineering. 2016. Vol. 126. P. 012019. doi: 10.1088/1757-899x/126/1/012019
17. Control loop tuning by thermal simulation applied to the laser transformation hardening with scanning optics process / Martínez S., Lamikiz A., Ukar E., Tabernero I., Arrizubieta I. // Applied Thermal Engineering. 2016. Vol. 98. P. 49–60. doi: 10.1016/j.applthermaleng.2015.12.037
18. Hardness Simulation of over-tempered Area During Laser Hardening Treatment / Martínez S., Lesyk D., Lamikiz A., Ukar E., Dzhemelinsky V. // Physics Procedia. 2016. Vol. 83. P. 1357–1366. doi: 10.1016/j.phpro.2016.08.143
19. Holovko L. F., Lukianenko S. O. Lazerni tekhnolohiyi ta kompiuterne modeliuvannia. Kyiv: Vistka, 2009. 296 p.
20. Mordyuk B. N., Prokopenko G. I. Ultrasonic impact peening for the surface properties' management // Journal of Sound and Vibration. 2007. Vol. 308, Issue 3-5. P. 855–866. doi: 10.1016/j.jsv.2007.03.054
21. Mordyuk B. N., Prokopenko G. I. Fatigue life improvement of α-titanium by novel ultrasonically assisted technique // Materials Science and Engineering: A. 2006. Vol. 437, Issue 2. P. 396–405. doi: 10.1016/j.msea.2006.07.119
22. Santhanakrishnan S., Kong F., Kovacevic R. An experimentally based thermo-kinetic phase transformation model for multi-pass laser heat treatment by using high power direct diode laser // The International Journal of Advanced Manufacturing Technology. 2012. Vol. 64, Issue 1-4. P. 219–238. doi: 10.1007/s00170-012-4029-z
23. An efficient model for laser surface hardening of hypo-eutectoid steels / Orazi L., Fortunato A., Cuccolini G., Tani G. // Applied Surface Science. 2010. Vol. 256, Issue 6. P. 1913–1919. doi: 10.1016/j.apsusc.2009.10.037
24. Jerniti A. G., Ouafi A. E., Barka N. Single Track Laser Surface Hardening Model for AISI 4340 Steel Using the Finite Element Method // Modeling and Numerical Simulation of Material Science. 2016. Vol. 06, Issue 02. P. 17–27. doi: 10.4236/mnsms.2016.62003
25. Kyryliv O. V., Nykyforchyn H. M., Kurzydlowski K. J. Evaluation of heat release in the process of pulsed mechanical hardening of titanium alloys // Materials Science. 2008. Vol. 44, Issue 3. P. 418–422. doi: 10.1007/s11003-008-9099-6